

Uncertainties quantification and modelling of different rheological models in estimation of pressure losses during drilling operation

Anawe P. A. L^{1*}, Folayan J. Adewale¹

¹ College of Engineering, Covenant University, Ota, Nigeria

*Corresponding author E-mail: paul.anawe@covenantuniversity.edu.ng

Abstract

The determination of pressure losses in the drill pipe and annulus with a very high degree of precision and accuracy is sacrosanct for proper pump operating conditions and correct bit nozzle sizes for maximum jet impact and forestalling of possible kicks and eventual blow outs during drilling operation. The two major uncertainties in pump pressure estimation that are being addressed in this research work are the flow behavior index (n) and the consistency index factor (k). It is in this light that the accuracy of various rheological models in predicting pump pressure losses as well as the uncertainties associated with each model was investigated.

In order to come by with a decisive conclusion, two synthetic based drilling fluids were used to form synthetic muds known as sample A and B respectively. Inference from results shows that the Newtonian model underestimated the pump pressure by 78.27% for sample A and 82.961% by for sample B. While the Bingham plastic model overestimated the total pump pressure by 100.70% for sample A and 48.17% for sample B. Three different power law rheological model approaches were used to obtain the flow behavior index and consistency factor of the drilling fluids. For the power law rheological model approaches, an underestimation error of 23.5743% was encountered for the Formular method for sample A while the proposed consistency index averaging method reduces the error to 14.9306%. The Graphical method showed a reasonable degree of accuracy with underestimation error of 5.6435%. Sample B showed an underestimation error of 47.8234% by using the power law formula method while the Consistency averaging method reduced the error to 20.7508. The graphical method showed an underestimation error of 0.4318%.

Keywords: Pressure Losses; Drill Pipe; Annulus; Power Law Model; Bingham Plastic Model; Consistency Index Averaging.

1. Introduction

Extremely large fluid pressures are generated in the well bore and tubular pipe strings by the presence of drilling mud or cement as a result of the following three well conditions. These are static condition in which both the well fluid and the central pipe string are at rest, a circulating operation in which fluids are being pumped down the central pipe string and up the annulus and lastly a tripping operation in which a central pipe string is being moved up or down through the fluid.

These pressure losses must be accurately measured and quantified because accurate estimation of the frictional pressure losses for non-Newtonian drilling fluids inside the annulus is quite important for determination of pump rates and selection of mud pump system during drilling operation [1]

However, modelling pressure losses resulting from fluid circulation and tripping operation are complicated by the non-Newtonian behavior of drilling muds and cement [2].

This non-Newtonian fluid behavior arises when the fluid viscosity is not constant but varies with the shear stress and prevailing shear rate or history [3]. The vivid description of this behavior has been explained by different rheologists [4-9]

In order to establish the relationship between flow pressure and flow rate, two fundamental flow regimes namely laminar flow and turbulent flow must be understood. While the former prevails at low

flow velocity with orderly flow, the latter is predominant at high velocity with a disordered flow.

In a bid to address the complexity associated with pressure estimations during drilling operations, various researchers have developed empirical and theoretical models for predicting pressure losses [10-11].

1.1. Materials and method

Two synthetic based drilling fluids were used to prepare synthetic based mud samples known as A and B respectively with the same mud components and composition. Sample A consist of Poly-alpha olefins (PAO) synthetic oil which was synthesized by the polymerization of ethylene. While sample B consist of Trans esterified Palm Kernel Oil (PKO).

1.2. Drilling fluid rheological models

The two basic models for describing the rheology of fluids are

- 1) The Newtonian model
- 2) The non-Newtonian model

The Newtonian model assumes that shear stress (τ) is directly proportional to the shear rate ($\dot{\gamma}$) and the constant of proportionality is the fluid viscosity (μ).

Pressure Estimation in Newtonian model

- a) For flow through the drill pipe

$$V_p = \frac{0.408q}{D_p^2} \text{ Ft/sec} \quad (1) \quad v_a = \frac{0.408q}{d_2^2 - d_1^2} \text{ (ft/sec)} \quad (19)$$

$$N_{Re} = \frac{928 D_p V_p \rho}{\mu_a} \quad (2) \quad \mu_a = \mu_p + \frac{5\tau_y(d_2-d_1)}{V_a} \quad (20)$$

Where $\mu_a = R_{300}$ (3) $N_{Re} = \frac{757(d_2-d_1) V_a \rho}{\mu_a}$ (21)

For laminal flow $N_{Re} < 2,100$ (4) $f_p = \frac{0.0791}{N_{Re}^{0.25}}$ (22)

$$f_p = \frac{16}{N_{Re}} \quad (5) \quad \left[\frac{dp}{dL} \right] = \frac{f_a V_a^2 \rho}{25.81(d_2-d_1)} \quad (23)$$

For turbulent flow

$$f_p = \frac{0.0791}{N_{Re}^{0.25}} \quad (6)$$

$$\left[\frac{dp}{dL} \right] = \frac{f_p V_p^2 \rho}{25.81 D_p} \quad (7)$$

b) For Annular flow

$$v_a = \frac{0.408q}{d_2^2 - d_1^2} \text{ (Ft/sec)} \quad (8)$$

$$N_{Re} = \frac{757(d_2-d_1) V_a \rho}{\mu_a} \quad (9)$$

$$\left[\frac{dp}{dL} \right] = \frac{f_a V_a^2 \rho}{25.81(d_2-d_1)} \quad (10)$$

2. The non-Newtonian model

Various non-Newtonian models used to characterize the behavior of drilling fluids includes but not limited to the following:

- a) Bingham Plastic model
- b) Power Law model
- c) Hershel Buckley Model
- d) Bingham Plastic Model

Fluids that follows Bingham's Plastic model, unlike a Newtonian fluid will not yield and begin to shear until a stress s applied that is large enough to break down the cohesive forces between the fluid particles.

Mathematically, for Bingham Plastic fluid,

$$\tau = \tau_y + \mu_p \gamma \quad (11)$$

$$\mu_p = \theta_{600} - \theta_{300} \quad (12)$$

$$\tau_y = \theta_{300} - \mu_p \quad (13)$$

Pressure Estimation in Bingham Plastic model

a) For flow through the drill pipe

$$V_p = \frac{0.408q}{D_p^2} \text{ Ft/sec} \quad (14)$$

$$\mu_a = \mu_p + \frac{5\tau_y D_p}{V_p} \quad (15)$$

$$N_{Re} = \frac{928 D_p V_p \rho}{\mu_a} \quad (16)$$

$$f_p = \frac{16}{N_{Re}} \quad (17)$$

$$\left[\frac{dp}{dL} \right] = \frac{f_p V_p^2 \rho}{25.81 D_p} \quad (18)$$

b) For Annular flow

a) Power Law model

The power law model is expressed as:

$$\tau = k \gamma^n \quad (24)$$

Where n is the fluid flow behaviour index which indicates the tendency of a fluid to shear thin and it is dimensionless, and k is the consistency coefficient which serves as the viscosity index of the system and the unit is $\text{lb}/100\text{ft}^2 \cdot \text{s}^n$. When $n < 1$, the fluid is shear thinning and when $n > 1$, the fluid is shear thickening [12].

The parameters k and n can be determined from a plot of $\log \tau$ versus $\log \gamma$ and the resulting straight line's intercept is $\log k$ and the slope is n .

It can also be determined from the following equations.

$$n = 3.32 \log \left(\frac{\theta_{600}}{\theta_{300}} \right) \quad (25)$$

$$k = \frac{\tau}{\gamma^n} = \frac{\theta_{600}}{1022^n} \text{ Or } K = \frac{510 R_{300}}{511^n} \text{ in } (\text{dyne} \cdot \text{sec}^n / \text{ft}^2) \quad (27)$$

Pressure Estimation in POWER LAW MODEL

a) For flow through the drill pipe

$$V_p = \frac{0.408q}{D_p^2} \text{ Ft/sec} \quad (28)$$

$$N_{Re} = \frac{89100 \rho V_p^{2-n}}{k} \left[\frac{0.0416 D_p}{3 + \frac{1}{n}} \right]^n \quad (29)$$

$$\left[\frac{dp}{dL} \right] = \frac{k V_p^n \left[3 + \frac{1}{n} \right]^n}{144000 D_p^{1+n}} \quad (30)$$

For laminal region,

$$N_{Re} \leq 3470 - 1370n \quad (31)$$

For turbulent region,

$$N_{Re} \geq 4270 - 1370n \quad (32)$$

b) For annular flow

$$v_a = \frac{0.408q}{d_2^2 - d_1^2} \text{ (Ft/sec)} \quad (33)$$

$$N_{Re} = \frac{109000 \rho V_a^{2-n}}{k} \left[\frac{0.0208 (d_2-d_1)}{2 + \frac{1}{n}} \right]^n \quad (34)$$

$$\left[\frac{dp}{dL} \right] = \frac{k V_a^n \left[2 + \frac{1}{n} \right]^n}{144000 (d_2-d_1)^{1+n}} \quad (35)$$

b) The Hershel- Buckley Model

It is an extension of the Bingham Plastic model to include shear rate dependence. Mathematically, it is expressed as:

$$\tau = \tau_{OH} + k_H \gamma^{n_H} \quad (36)$$

Where γ is the shear rate (s^{-1}), τ is the shear stress (Pa), nH is the flow behaviour index (dimensionless), kH is the consistency index and τ_0H is the yield stress.

A plot of $\log(\tau - \tau_0H)$ versus $\log(\gamma)$ will result in a straight line with intercept $\log kH$ and slope nH respectively.

Pressure Estimation in HERSHEY- BUCKLEY MODEL

(a) For flow through the drill pipe

$$V_p = \frac{0.408q}{D_p^2} Ft/sec \quad (37)$$

$$N_{Re} = \left[\frac{2(3n+1)}{n} \right] \left\{ \frac{\rho V_p^{2-n} \left(\frac{Dp}{2}\right)^n}{\tau_0 \left(\frac{Dp}{2V_p}\right)^n + k \left[\frac{3n+1}{nC_c}\right]^n} \right\} \quad (38)$$

$$N_{Rec} = \left[\frac{4(3n+1)}{ny} \right]^{1-z} \quad (39)$$

$$y = \frac{\log n + 3.93}{50} \quad (40)$$

$$z = \frac{1.75 - \log n}{7} \quad (41)$$

$$C_c = 1 - \left[\frac{1}{2n+1} \right] \left\{ \frac{\tau_0}{\tau_0 + k \left[\frac{(3n+1)q}{n\pi \left(\frac{Dp}{2}\right)^3} \right]^n} \right\} \quad (42)$$

$$\left[\frac{dp}{dL} \right] = \frac{4k}{14400D_p} \left\{ \left(\frac{\tau_0}{k} \right) + \left(\left[\frac{3n+1}{nC_c} \right] \left[\frac{8q}{\pi D_p^3} \right] \right)^n \right\} \quad (43)$$

For Annular Flow

$$v_a = \frac{0.408q}{d_2^2 - d_1^2} (Ft/sec) \quad (44)$$

$$N_{Re} = \left[\frac{4(2n+1)}{n} \right] \left\{ \frac{\rho V_a^{2-n} \left(\frac{d_2-d_1}{2}\right)^n}{\tau_0 \left(\frac{d_2-d_1}{2V_a}\right)^n + k \left[\frac{2(2n+1)}{nC_a}\right]^n} \right\} \quad (45)$$

$$N_{Rec} = \left[\frac{8(2n+1)}{ny} \right]^{1-z} \quad (46)$$

$$\left[\frac{dp}{dL} \right] = \frac{4k}{14400(d_2-d_1)} \left\{ \left(\frac{\tau_0}{k} \right) + \left(\left[\frac{16(2n+1)}{nC_a(d_2-d_1)} \right] \left[\frac{q}{\pi(d_2^2-d_1^2)} \right] \right)^n \right\} \quad (47)$$

$$C_a = 1 - \left[\frac{1}{n+1} \right] \left\{ \frac{\tau_0}{\tau_0 + k \left[\frac{2(2n+1)}{n \left(\frac{d_2-d_1}{2}\right)} \right] + \left[\frac{q}{\pi \left(\frac{d_2^2-d_1^2}{2}\right)} \right]^n} \right\} \quad (48)$$

$$\Delta P = \left[\frac{dp}{dL} \right] \Delta L \quad (49)$$

Pressure loss in the bit.

$$\Delta P = \frac{156\rho q^2}{[D_{N1}^2 + D_{N2}^2 + D_{N3}^2]^2} \quad (50)$$

3. Results and discussion

3.1. Sample A flow behaviour analysis

The result from direct viscometer readings for Mud Sample A is presented in table 1 below

Table 1: Viscometer Readings for SAMPLE A

Speed (RPM)	Dial Reading(lb/100ft ²)	Shear rate (s ⁻¹)
600	78	1022
300	53	511
200	41	340.60
100	28	170.30
60	19	102.18
30	14	51.09
6	10	10.22
3	8	5.11

Note: Mud Density Is 9.50ppg

3.1.1. Model parameters determination for sample A using the power law model

a) Using power law rheology equation

The flow behavior index is estimated by using equation 25 as 0.5572 and the consistency factor is obtained by using equation 27 as 1.64146 (lb/100ft²sⁿ) or 0.837mpasⁿ or 837 (dyne.secⁿ/ft²).

b) Using Graphical Method.

The power law rheological model parameters (n and k) were obtained by a plot of $\log \tau$ versus $\log \gamma$ as shown in Figure. 1 below which gives a straight line with slope n and intercept $\log k$.

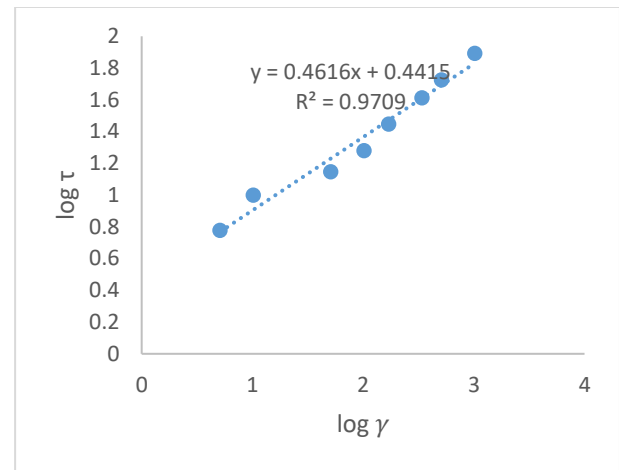


Fig. 1: Power Law Rheogram for Sample A.

Hence, from Figure 1, n is 0.4616 and k is 2.7638 (lb/100ft²sⁿ) or 1.4095mpasⁿ or 1409.5 (dyne.secⁿ/ft²).

(c) Consistency Index Averaging.

The result of each consistency index at the corresponding values of shear rate and shear stress as calculated by equation 26 is given in Table 2 below.

Table 2: Consistency Index at the Corresponding Values of Shear Rate and Shear Stress for Sample A

Speed (RPM)	Stress(lb/100ft ²)	shear rate (s ⁻¹)	n	k (lb/100ft ² s ⁿ)	K (mpas ⁿ)
600	78	1022	0.557	1.641453	0.83714
			2		1
300	53	511	0.557	1.641133	0.83697
			2		8
200	41	340.6	0.557	1.591538	0.81168
			2		5
100	28	170.3	0.557	1.599283	0.81563
			2		4
60	19	102.1	0.557	1.442563	0.73570
			2		7
30	14	51.09	0.557	1.564023	0.79765
			2		2
6	10	10.21	0.557	2.738932	1.39685
			2		6
3	6	5.109	0.557	2.418057	1.23320
			2		9

From table 2, Average K is $1.8296(lb/100ft^2s^n)$ or 0.9331 $mpas^n$ or 933 $(dyne.sec^n/ft^2)$.

3.1.2. Hershel-buckley model

The flow behaviour index (n_H) and consistency index (k_H) were obtained by a plot of $\log(\tau - \tau_{0H})$ against $\log \gamma$ which gives a straight line as shown in Figure 2.

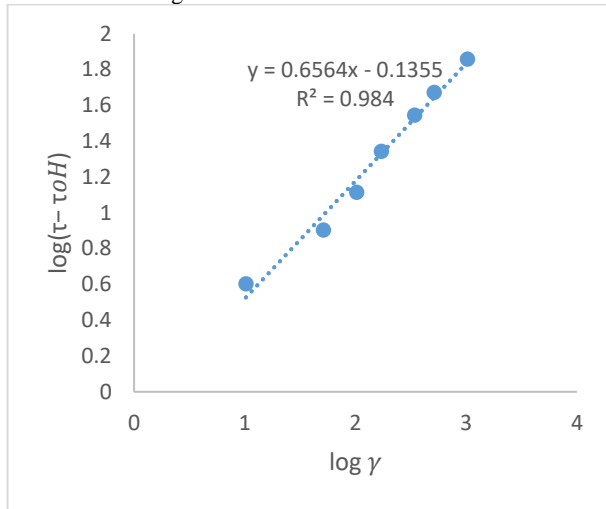


Fig. 2: Hershel-Buckley Rheogram for SAMPLE A.

From Figure 2, n_H is 0.6564 and k_H is 0.7320 $(lb/100ft^2s^n)$

3.2. Sample B flow behaviour analysis

Similarly, the result from direct viscometer readings for Mud Sample B is presented in table 3 below

Table 3: Viscometer Readings for SAMPLE B

Speed (RPM)	Dial Reading(lb/100ft ²)	Shear rate (s ⁻¹)
600	88	1022
300	57	511
200	46	340.60
100	32	170.30
60	24.50	102.18
30	17	51.09
6	13	10.22
3	10	5.11

Note: Mud Density Is 10.00ppg

3.2.1. Model parameters determination for sample B using the power law model

a) Using power law rheology equation
The flow behavior index is estimated by using equation 25 as 0.6265 and the consistency factor is obtained by using equation 27 as $1.1456(lb/100ft^2s^n)$ or $0.584.277mpas^n$ or $584.277(dyne.sec^n/ft^2)$

b) Using Graphical Method.
The power law rheological model parameters (n and k) were obtained by a plot of $\log \tau$ versus $\log \gamma$ as shown in Figure.3 below which gives a straight line with slope n and intercept $\log k$.

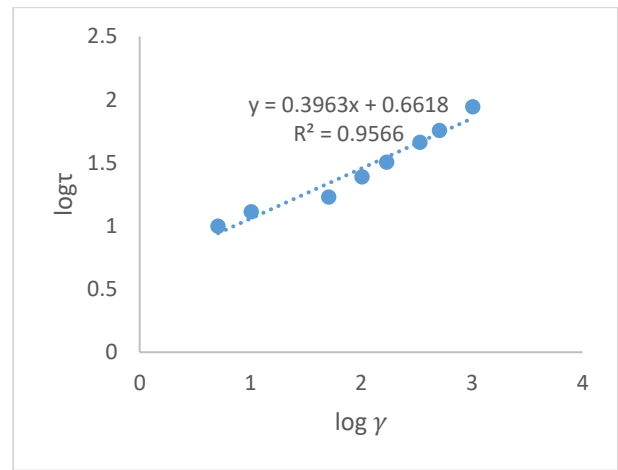


Fig. 3: Power Law Rheogram for Sample B

Hence, from Figure 3, n is 0.3963 and k is 4.5899 $(lb/100ft^2s^n)$ or 0.23408 $mpas^n$ or 2340.8 $(dyne.sec^n/ft^2)$.

c) Consistency Index Averaging.

The result of each consistency index at the corresponding values of shear rate and shear stress as calculated by equation 27 is given in Table 4 below.

Table 4: Consistency Index at the Corresponding Values of Shear Rate and Shear Stress for Sample B

Speed (RP M)	Stress(lb/100ft ²)	shear rate (s ⁻¹)	n	k $(\frac{lb}{100ft^2s^n})$	K (mpas ⁿ)
600	88	1022	0.6265	1.145676	0.584295
300	57	511	0.6265	1.145643	0.584278
200	46	340.6	0.6265	1.192083	0.607962
100	32	170.3	0.6265	1.280248	0.652926
60	24.5	102.1	0.6265	1.34989	0.688444
30	17	51.09	0.6265	1.446027	0.737474
6	13	10.21	0.6265	3.030928	1.545773
3	10	5.109	0.6265	3.599379	1.835683

From Table 4,the Average K is $1.7737(lb/100ft^2s^n)$ or 0.9046 $mpas^n$ or 904.6 $(dyne.sec^n/ft^2)$.

3.2.2. Hershel-buckley model

The flow behaviour index (n_H) and consistency index (k_H) were obtained by a plot of $\log(\tau - \tau_{0H})$ against $\log \gamma$ which gives a straight line as shown in Figure 4.

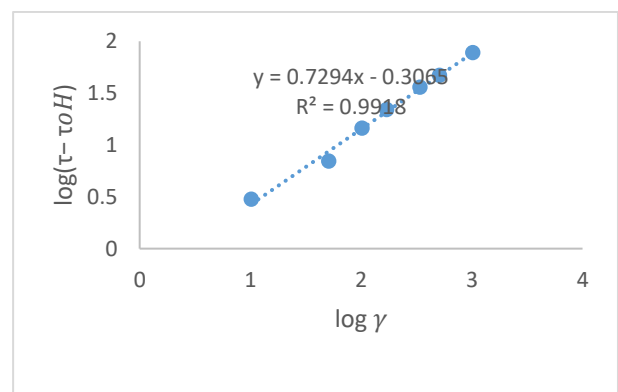


Fig. 4: Hershel-Buckley Rheogram for SAMPLE B

From Figure 4, n_H is 0.7294 and k_H is 0.4937 ($lb/100ft^2s^n$)
N/A: NOT APPLICABLE, AVG= AVERAGING

From table 5, the Herschel Buckley rheological model has a flow behavior index of 0.6564 for SAMPLE A and 0.7294 for sample B which indicates that the fluid is shear thinning but with a higher degree of shear thinning ability in sample A because it has lesser value of flow behavior index. The same scenario is experienced in power law model with sample A being more shear thinning than sample B.

3.3. Flow behaviour characteristics analysis

From table 6, for Newtonian model, the flow in sample A is more laminar than flow in sample B. In addition, for Bingham plastic model, a more laminar flow is experienced in sample A than sample B. This is largely due to different base fluid properties of each sample most especially, the viscosity. From table 7, the power law model Reynolds number N_{RE} obtained by using the formula approach is more than the formula and consistency-averaging approaches for mud flow through the pipe for the two mud samples. This translates to the fact that the formula approach falsely represents a lesser laminar flow than the other two approaches (Graphical and Consistency index averaging). Table 8 represents mud flow behavior characteristics in the annulus. The Newtonian model assumed a less laminar flow than the Herschel–Buckley and Bingham plastic model for the two mud samples.

N/A: NOT APPLICABLE, AVG= AVERAGING

Table 5: Summary of Non-Newtonian Rheological Parameters

Rheological Model	Flow Behaviour Index (N)	Consistency Factor ($lb/100ft^2s^n$) (K)	Consistency Factor (K) ($dyne.sec^n/ft^2$)	Yield Stress (τ) $lb/100ft^2$	Plastic Viscosity (μ_p) $lb/100ft^2$
Sample A					
Bingham Plastic Model	N/A	N/A	N/A	28	25
Herschel Buckley Model	0.6564	0.7320	373.30	6.00	25
Power Law Model					
Formular Approach	0.5572	1.6414	837	28	25
Graphical Approach	0.4616	2.7638	1409.5	28	25
Consistency Index Avg	0.5572	1.866	933.1	28	25
Sample B					
Bingham Plastic Model	N/A	N/A	N/A	26	31
Herschel Buckley Model	0.7294	0.4937	251.787	10	31
Power Law Model					
Formular Approach	0.6265	1.1456	584.277	26	31
Graphical Approach	0.3963	4.5899	2340.831	26	31
Consistency Index Avg	0.6265	1.7737	904.60	26	31

Table 6: Flow Behavior Characteristics of Mud Flow through the Drill Pipe

Rheological Model	Pipe Velocity V_p (Ft/Sec)	Reynolds Number N_{RE}	N_{RE} Critical Constant	Critical N_{RE}	Flow Regime	Fanning Friction Factor
Sample A						
Newtonian Model	2.015	1378.26	N/A	> 2100	Laminar	0.01161
Bingham Plastic Model	2.015	236	N/A	> 2100	Laminar	0.0676
Herschel Buckley Model	2.015	151.772	0.566	1931	Laminar	-
Sample B						
Newtonian Model	2.015	1476.25	N/A	> 2100	Laminar	0.0108
Bingham Plastic Model	2.015	261.75	N/A	> 2100	Laminar	0.0611
Herschel Buckley Model	2.015	133.025	0.7764	1721.18	Laminar	-----

From table 9, it can be deduced that the power law rheological model through formular approach showed that the flow is less laminar inside the annulus than the graphical and consistency index averaging approach.

3.4. Pressure analyses

The data from [13] as shown in appendix A, were used to validate the pressure analysis. The pressure losses inside the pipe flow, bit and annulus for the mud samples A and B are shown in table 10. It can be inferred that more pressure is lost in the drill pipe than in the annulus. The lowest pressure loss was experienced in the bit for all the mud samples.

Also, From Table 10, The Bingham plastic rheological model showed the highest values of pressure losses for flow through the pipe and the annulus for the two mud samples. While the Newtonian model showed the least values of pressure losses for flow through the pipe and annulus for the mud samples.

3.5. Model pressure performance analysis

According to [14-16], the Herschel Buckley is the most accurate in describing rheological behavior of drilling muds, Hence, the degree of deviation of pressure losses for each model was measured by comparing with pressure losses predicted by Herschel Buckley model for the mud samples.

Table 7: Flow Behaviour Characteristics of Mud Flow through the Drill Pipe for Different Power Law Model Approaches

Power Law Model	Pipe Velocity V_p (Ft/Sec)	Reynolds Number N_{RE}	Laminar Critical N_{RE}	Turbulent Critical N_{RE}	Flow Regime
Sample A					
Formular Approach	2.015	456.08	2706.636	3506.636	Laminar
Graphical Approach	2.015	381.524	2837.608	3637.608	Laminar
Consistency Index Avg	2.015	409.08	2706.636	3506.636	Laminar
Sample B					
Formular Approach	2.015	537.388	2611.695	3411.695	Laminar
Graphical Approach	2.015	306	2927.07	3727.07	Laminar
Consistency Index Avg	2.015	347.046	2611.695	3411.695	Laminar

Table 8: Flow Behavior Characteristic of Mud Flow through the Annulus

Rheological Model	Pipe Velocity V_a (Ft/Sec)	Reynolds Number N_{RE}	N_{RE} Critical Constant	Critical N_{RE}	Flow Regime	Fanning Friction Factor
Sample A						
Newtonian Model	0.4547	352	N/A	> 2100	Laminar	0.0454
Bingham Plastic Model	0.4547	10.4715	N/A	> 2100	Laminar	1.528
Herschel Buckley Model	0.4547	18.140	0.6391	3610.63	Laminar	-
Sample B						
Newtonian Model	0.4547	344.872	N/A	> 2100	Laminar	0.0108
Bingham Plastic Model	0.4547	11.8150	N/A	> 2100	Laminar	0.0611
Herschel Buckley Model	0.4547	14.0395	0.5615	3109.88	Laminar	-

Table 9: Flow Behavior Characteristic of Mud Flow through the Annulus for Different Power Law Model Approaches

Power Law Model	Pipe Velocity V_p (Ft/Sec)	Reynolds Number N_{RE}	Laminar Critical N_{RE}	Turbulent Critical N_{RE}	Flow Regime
Sample A					
Formular Approach	0.4547	57.5819	2706.636	3506.636	Laminar
Graphical Approach	0.4547	42.304	2837.608	3637.608	Laminar
Consistency Index Avg	0.4547	51.650	2706.636	3506.636	Laminar
Sample B					
Formular Approach	0.4547	74.632	2611.695	3411.695	Laminar
Graphical Approach	0.4547	31.1074	2927.07	3727.07	Laminar
Consistency Index Avg	0.4547	48.206	2611.695	3411.695	Laminar

Table 10: Pressure Analyses

Rheological Model	Pipe Flow	Annular Flow	Bit Nozzle	Total Pressure		
Sample A	Pressure Gradient $\left[\frac{dP}{dL}\right]$ (Psi/Ft)	Pressure Loss(Δpds) (Psi)	Pressure Gradient $\left[\frac{dP}{dL}\right]$ (Psi/Ft)	Pressure Loss(Δpa) (Psi)	Pressure Loss(Δpb) (Psi)	Pump Pressure (ΔPT)(Psi)
Newtonian	0.003855	47.960	0.0006051	7.5272	2.6790	58.1662
Bingham Plastic	0.0224	278.656	0.02036	253.28	2.6790	534.615
Herschel Buckley	0.1453	180.7532	0.006664	82.894	2.6790	266.380
Power Law						
Formular Approach	0.01163	144.662	0.004521	56.2419	2.6790	203.5828
Graphical Approach	0.01390	172.916	0.006154	76.556	2.6790	252.15
Consistency Index Avg	0.01296	161.24	0.005039	62.688	2.6790	226.6078
Sample B	Pressure Gradient $\left[\frac{dP}{dL}\right]$ (Psi/Ft)	Pressure Loss(Δpds) (Psi)	Pressure Gradient $\left[\frac{dP}{dL}\right]$ (Psi/Ft)	Pressure Loss(Δpa) (Psi)	Pressure Loss(Δpb) (Psi)	Pump Pressure (ΔPT)(Psi)
Newtonian	0.003789	47.133	0.000651	8.095	2.82	58.048
Bingham Plastic	0.02136	265.712	0.0190	236.29	2.82	504.831
Herschel	0.01470	182.902	0.01245	154.95	2.82	340.672

Buckley Power Law Formular Approach	0.0104	129.241	0.003673	45.69	2.82	177.751
Graphical Approach	0.018228	226.759	0.008812	109.622	2.82	339.201
Consistency Index Avg	0.01608	200.0352	0.005399	67.16	2.82	26.98

Table 11: Percentage Error in Pump Pressure for Each Rheological Model

Model Mud Sample	Newtonian	Bingham Plastic	Plrm Formular	Plrm Graphical	Plrm K Avg
Sample A	-78.273	+100.70	-23.5743	-5.6435	-14.9306
Sample B	-82.961	+48.1868	-47.8234	-0.4318	-20.7508

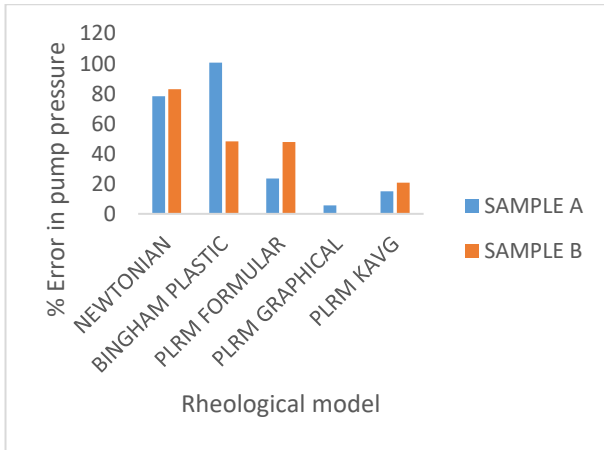


Fig. 5: Percentage Error in Pump Pressure for Each Rheological Model.

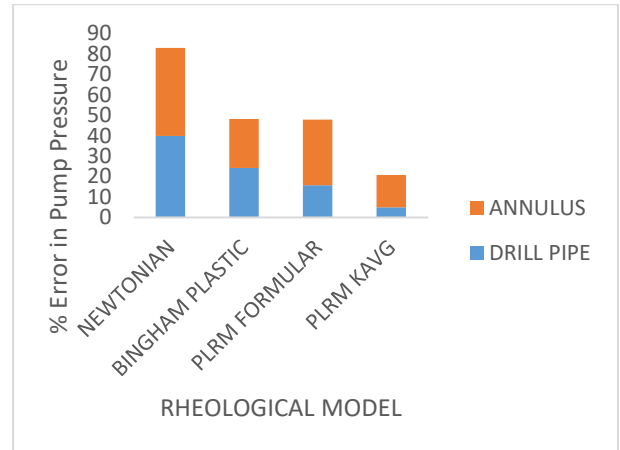


Fig. 7: Relative Contribution of Drill Pipe and Annulus Pressure Errors to the Total Pump Pressure Error for Sample B.

From table 11 and figure 5, the Newtonian model underestimated the pump pressure by 78.27% for sample A and 82.961% by for sample B. While the Bingham plastic model overestimated the total pump pressure by 100.70% for sample A and 48.17% for sample B. The result obtained from the Bingham plastic model is in agreement with the work of [17] where it was recorded that the model overestimates pressure losses. For the power law rheological model approaches for sample A, an underestimation error of 23.5743% was encountered for the Formular method while the proposed consistency index averaging method reduces the error to 14.9306%. The Graphical method showed a reasonable degree of accuracy with underestimation error of 5.6435%. Similarly, from Table 11 and Figure 5, sample B showed an underestimation error of 47.8234% by using the power law formular method while the Consistency averaging method reduced the error to 20.7508%. The graphical method showed an underestimation error of 0.4318%.

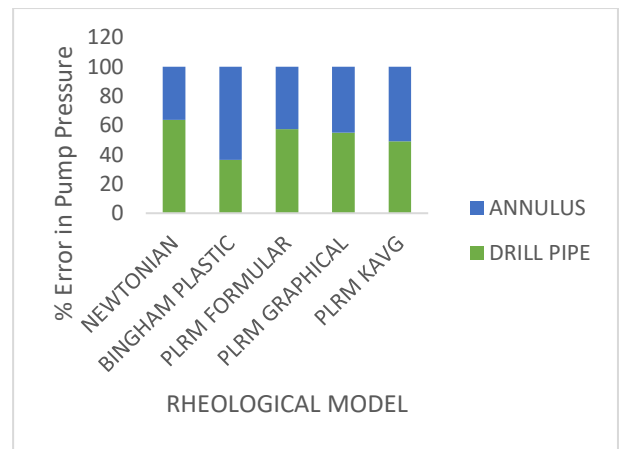


Fig. 8: Percentage Contribution of Drill Pipe and Annulus Pressure Errors to the Total Pump Pressure Error for Sample A.

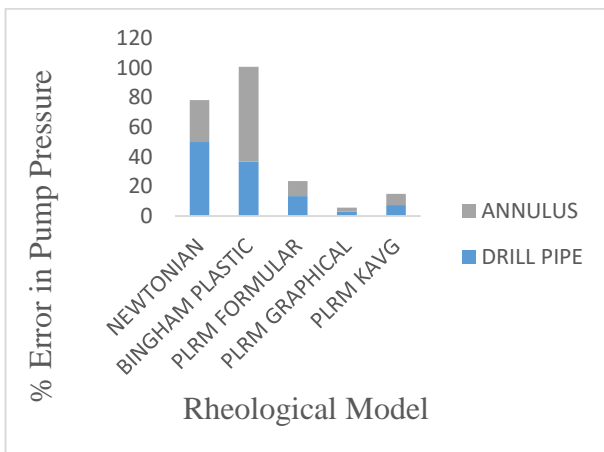


Fig. 6: Relative Contribution of Drill Pipe and Annulus Pressure Errors to the Total Pump Pressure Error for Sample A.

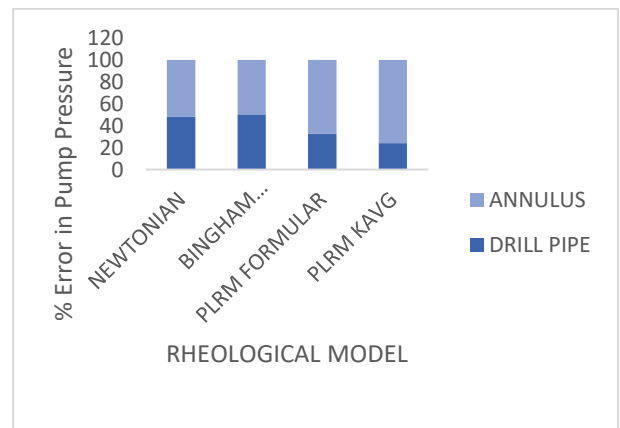


Fig. 9: Percentage Contribution of Drill Pipe and Annulus Pressure Errors to the Total Pump Pressure Error for Sample B.

From figure 6 and 8, it can be deduced that larger error was contributed by drill pipe from Newtonian, Power law formula method and Graphical method while the annulus contributed a relatively larger error to total pump pressure error from Bingham plastic and consistency index averaging method. A reverse scenario was observed for sample B as shown in Figure 7 and 9.

4. Conclusion

The following conclusions can be drawn from experimentation and model performance analysis.

- The Newtonian model underestimated the pump pressure by 78.27% for sample A and 82.961% for sample B.
- The Bingham plastic model overestimated the total pump pressure by 100.70% for sample A and 48.17% for sample B.
- The power law rheological model formula approach underestimated the pump pressure by 23.5743% for sample A and 47.8234% for sample B.
- The proposed consistency index averaging method of power law model reduces the formula method error to 14.9306% for sample A and 20.7508% for sample B.
- The Graphical method showed a reasonable degree of accuracy with underestimation error of 5.6435% and 0.4318% for sample A and B respectively.

References

- [1] Sorgun, M., and Ozbayoglu M. E. (2011). Predicting Frictional Pressure Loss During Horizontal Drilling for Non-Newtonian Fluids. *Energy Sources, Part A: Recovery, Utilization, and Environmental Effects*. 33:7, pp 631-640. <https://doi.org/10.1080/15567030903226264>.
- [2] Bourgoyne, A.T., Millheim, K.K., Chenevert, M.E and Young F.S (1991). Applied Drilling Engineering, SPE, and Richardson, Texas Volume 2.
- [3] Steffe, J. F (1996). Rheological Methods in Food Process Engineering. Sixth Edition. Freeman press. East Lansing USA. ISBN 0-9632036-1-4.
- [4] Bingham, E.C. (1922). Fluidity and Plasticity. MC Graw-hill, New York.
- [5] Herschel, W.H. and Buckley, R. (1926.) Konsistenzmessungen von Gummi Benzollösungen. *Kolloid Z* 39; pp.291-300.
- [6] Casson, M. (1959). The Rheology of Disperse Systems. Pergamon press, London.
- [7] Dodge, D.G., and Metzner, A.B (1959). Turbulent flow of non-Newtonian Systems. *AICHE.J.* 5,189. <https://doi.org/10.1002/aic.690050214>.
- [8] Hanks, R.W., and Pratt, D.R (1967). On the flow of Bingham Plastic Slurries in Pipes and Between Parallel Plates. *Society of Petroleum Engineers Journal*. Pp 342-346 <https://doi.org/10.2118/1682-PA>.
- [9] Robertson R.E., and Stiff, H.A (1976). An Improved Mathematical Model for Relating Shear Stress to Shear Rate in Drilling Fluids and Cement Slurries. *Trans, AIME* ,26, pp 31
- [10] Sample, K.J and Bourgoyne, A.T, (1978). Development of Improved Laboratory and Field Procedures for Determining the Carrying Capacity of Drilling Fluids. SPE PAPER 7497, Presented at Society of Petroleum Engineers Annual Technical Conference and Exhibition Houston.
- [11] Burkhardt J.A (1961). Well Bore Pressure Surges Produced by Pipe Movement. *Journal of petroleum technology*. 595-60 trans AIME 222
- [12] Reiner, M. (1926). *Kolloid Z.* 39, pp. 80-87
- [13] White, W and Zamora, M (1997). Downhole Measurements of Synthetic Based Drilling Fluid in an Offshore Well Quantifying Dynamic Pressure and Temperature Distribution. Paper SPE 35057 Presented at the 1997 Society of Petroleum Engineers Drilling Conference, New Orleans.
- [14] Hemphill, T.; Campos, W.; and Pilehvari, A (1993). Yield Power Law Model more accurately predicts Mud Rheology". *Oil and Gas Journal*, 91, pp .34
- [15] Katarin, S (2004). The Role of Different Rheological Models in Accuracy of Pressure Loss Prediction. Vol 16, pp 85-89, Rudarsko-geolosko-naftini Zbornik. Zagreb.
- [16] Folayan, J. A, Anawe, P.A. L, Abioye, P.O and Elehinafe F.B (2017). Selecting the Most Appropriate Model for Rheological Characterization of Synthetic Based Drilling Mud. *International Journal of Applied Engineering Research*. Vol 12. Pp 7614-7629.
- [17] Langlinais, J. P, Bourgoyne, A. T and Holden W. R (1983). Frictional Pressure Losses for the Flow of Drilling Mud and Mud/Gas Mixtures. Society of Petroleum Engineers, paper 11993 presented at the annual technical conference, San Francisco.

Appendix A

Data from White and Zamora (1997)
 Drillpipe-5 in. 19.5 S-135 w/4.5
 IF (675in.x 3in. connection)
 D1= 5 in, Dp =4.5 in
 Casing 11 7/8 in.x10.711 in.,
 D2=10.711 in.
 Length of well= 12440ft
 q1=100 GPM
 Bit: 10 5/8 in. w/3: 28/32 in. jets
 $\Delta P_s=0$